

Impact of a reduced layout of the ATLAS pixel detector on the channel $t\bar{t}H$, $H \rightarrow b\bar{b}$

(preliminary results, waiting for a final b-tagging
parametrization)

J. Cammin¹

D. Costanzo²

1. *Physikalisches Institut der Universität Bonn, Nussallee 12, D-53115 Bonn*

2. *Lawrence Berkeley Laboratory, 1 Cyclotron Rd, Berkeley, CA 94720*

Abstract

The performance of the ATLAS detector for the reconstruction of the $t\bar{t}H$ signal is studied in this note emphasizing the role played by the pixel sub-system in tagging b-jets. The analysis proposed in the PHYSICS TDR has been repeated using the ATLFAST simulation in its FORTRAN and the ATHENA versions. Four different scenarios for the b-tagging have been considered, depending on the expected design and performance of the pixel sub-system. The degradation of the statistical significance obtained for 30 fb^{-1} with a reduced pixel layout has been quantified.

July 30, 2002

DRAFT

Version 0.4

¹Jochen.Cammin@cern.ch

²DCostanzo@lbl.gov

1 Introduction

The discovery of the Higgs boson is one of the major goals in the physics program of the upcoming LHC. The expected sensitivity of the LHC experiments to the Higgs boson covers a large mass range, from less than 100 GeV up to 1 TeV. The design of the ATLAS detector will permit the search for the Higgs boson in a large variety of production processes and decay modes. In the mass region below 135 GeV the Higgs boson decays predominately into $b\bar{b}$. The direct production, $gg \rightarrow H \rightarrow b\bar{b}$, has the largest cross section, but this channel is flooded by a huge QCD background. To suppress this background efficiently, one needs to turn to rare Higgs decay modes with a clean signature, for instance $H \rightarrow \gamma\gamma$, or to other production modes with a signature which is substantially different from the QCD background, *e.g.* the production of a Higgs boson in association with other particles.

It has been shown in the PHYSICS TDR [1] that the Higgs boson can be observed at masses below about 130 GeV in its dominant decay mode $H \rightarrow b\bar{b}$. The observation of this decay channel is possible in the production of a Higgs boson accompanied by a pair of top quarks, $pp \rightarrow t\bar{t}H$, with a predicted significance of 3.6 for $m_H = 120$ GeV and $\mathcal{L} = 30 \text{ fb}^{-1}$. Each top-quark decays almost exclusively into a W boson and a b-quark. One W is required to decay into an electron or a muon plus the respective neutrino, and the other W to decay hadronically. This yields 6 jets, 1 lepton and missing momentum in the detector. Four of the 6 jets must be labeled as b-jets in order to suppress the large background from top-pairs with additional jets from initial or final state gluon radiation. This requirement demands excellent performance of the ATLAS detector in finding true b-jets and keeping the rate of mistagged c- and light-jets low. The pixel sub-system of the Inner Detector is a crucial ingredient for the recognition of displaced vertices.

In this note we investigate the effect of a possible reduced layout of the pixel sub-system on the statistical significance of the $t\bar{t}H$ channel. The note is organized as follows: In Section 2 we describe the reconstruction and analysis procedure. Section 3 quantifies the impact of a reduced layout and Section 4 summarizes the results.

Convention: We use the term ‘ $t\bar{t} + X$ ’ to denote both the reducible and the irreducible contribution of the QCD-top-pair background, ‘ $t\bar{t}b\bar{b}$ ’ for the irreducible component and ‘ $t\bar{t}jj$ ’ for the reducible contribution where the jets (‘ jj ’) do not originate from real b-quarks. Therefore, in this definition, $t\bar{t}b\bar{b}$ and $t\bar{t}jj$ are complementary, and $t\bar{t} + X = t\bar{t}b\bar{b} \cup t\bar{t}jj$.

2 Analysis

In this work we closely follow the procedure described in the ATLAS PHYSICS TDR [1] and in [5] to quantify the impact of the present pixel sub-system layout and its expected performance.

Both the semileptonic and the hadronic top decays are fully reconstructed to reduce the combinatoric choices of the b-jets assigned to the Higgs decay. The main background originates from top-pair production together with additional jets from initial or final state gluon radiation. When those additional jets originate from a $b\bar{b}$ pair the background is irreducible, while the amount of background events with extra-jets originating from light- or c-quarks depends crucially on the rejection against light- or c-jets, *i.e.* on the detector performance.

2.1 Monte Carlo samples and cross sections

Both the signal and the $t\bar{t} + X$ (QCD) background samples were generated with PYTHIA 6.203. The irreducible $t\bar{t}b\bar{b}$ (QCD) background was also simulated using the matrix element (ME) calculations with ACERMC [3]. Both the graphs with the exchange of gluons (QCD) and of electroweak gauge bosons ($Z/\gamma/W$) have been considered. The decays of the top quarks were forced to have one charged lepton (e or μ) in the final state.

The signal cross section has been calculated with the hqq program [7], with the renormalization and factorization scale set to $Q_{\text{QCD}}^2 = (m_t + m_H/2)^2$ ($m_H = 120$ GeV). This scale was proposed in [9] as a “natural” choice for this process.

Only those backgrounds containing a pair of top quarks (plus additional particles) have been considered, since other backgrounds are almost negligible. At the generator level this background has been split into a reducible component and an irreducible component. The reducible component from $t\bar{t} + X$ has been generated with PYTHIA requiring less than four b-quarks in the final state, while the irreducible component from $t\bar{t}b\bar{b}$ has been calculated using ACERMC [3] to generate the ME events which were then interfaced to PYTHIA for the showering process. This procedure has been defined to avoid double counting of the irreducible $t\bar{t}b\bar{b}$ events generated by PYTHIA with subsequent showering. PYTHIA events with four or more final state b-quarks have been compared to the $t\bar{t}b\bar{b}$ (QCD) prediction from ACERMC.

The cross section values used in this study are listed in Table 1 together with the ones used in the PHYSICS TDR. The factor “BR” includes the branching ratio for the final state $\ell\nu b$ $j\bar{j}b$ $b\bar{b}$ in case of the signal, and $\ell\nu b$ $j\bar{j}b$ in case of the background. The branching ratio for $t\bar{t} \rightarrow \ell\nu b$ $j\bar{j}b$ was taken to be 0.2913, and for $H \rightarrow b\bar{b}$ a value of 0.70 was used for $m_H = 120$ GeV [2, 7].

Two different approaches for the event generation and the multi-interaction settings were used:

Process	σ (pb)	$\sigma \times \text{BR}$ (pb)	TDR: $\sigma \times \text{BR}$ (pb)
$t\bar{t}H$	0.55	0.11	0.14
$t\bar{t} + X$ (PYTHIA)	490.	143.	170.
$t\bar{t}b\bar{b}$ (ACERMC QCD)	8.1	2.35	N/A
$t\bar{t}b\bar{b}$ (ACERMC EW)	0.90	0.26	N/A

Table 1: Cross sections for signal and background.

- Default PYTHIA multi-interaction scheme, $\text{MSTP}(82) = 1$. This setting was used with the FORTRAN version of ATLFAST;
- Multi-interaction scheme assuming a varying impact parameter and a hadronic matter overlap, $\text{MSTP}(82) = 4$ and $\text{PARP}(82) = 2.2$. This scheme is used by CDF [4] to model the minimum bias events. This setting was used for the event simulation in the ATHENA framework.

The FORTRAN and the ATHENA simulation frameworks are known to give comparable results³, however a signal event sample was generated with ATHENA using the PYTHIA default multi-interaction scheme and some distribution were compared and found to be in a good agreement. As an example, Fig. 1 shows the b-jet multiplicity distributions in $t\bar{t}H$ events as obtained with t

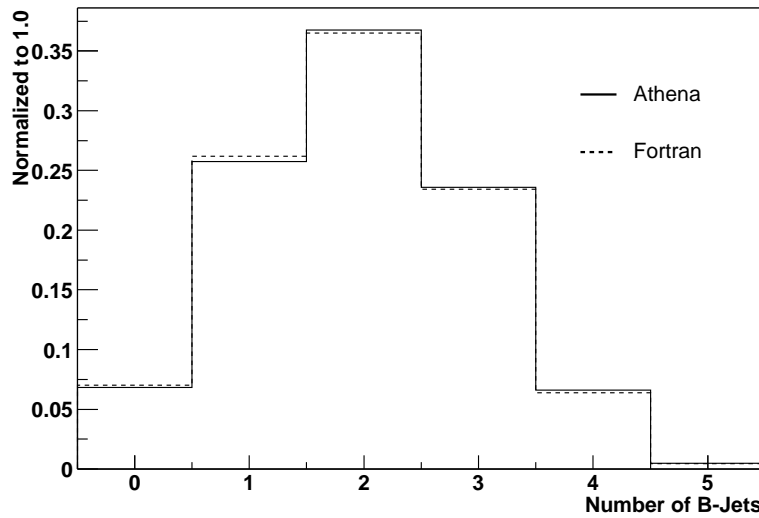


Figure 1: Number of b-jets in signal events obtained with the FORTRAN and ATHENA version of ATLFAST, using the same setting for the multi-interactions.

³See examples at <http://www.hepl.ucl.ac.uk/atlfast/AtlfastPhysics.html>

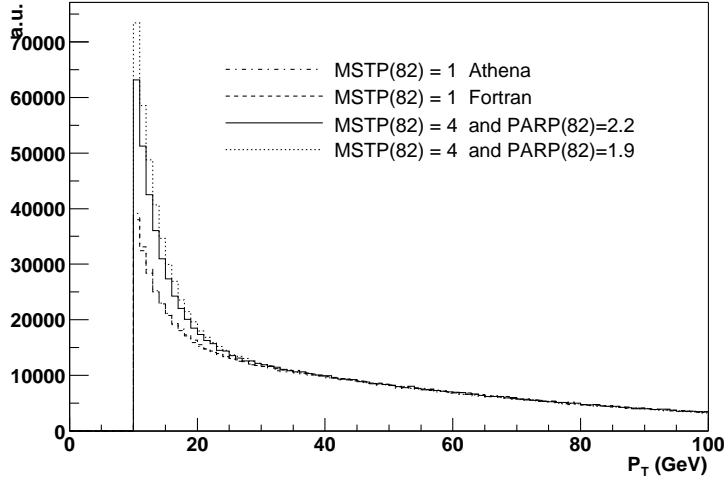


Figure 2: Inclusive p_T of all the jets in $t\bar{t}H$ events. The different lines correspond to different choices for the multi-interaction scheme.

The difference between the two multi-interaction schemes is depicted in Fig. 2, where the p_T distribution of all the jets in $t\bar{t}H$ events is shown. It can be seen that the multi-interaction scheme corresponding to $\text{MSTP}(82) = 4$ causes a higher multiplicity of low- p_T jet as it is expected from Ref. [4]; the dependence of the jet multiplicity on the cut-off parameter – $\text{PARP}(82)$ – for this scheme is also shown. Two values for the cut-off parameter were used: 1.9, which is the PYTHIA default and 2.2, which is the value suggested in Ref. [4]. The latter choice has been used throughout this work for the analysis in the ATHENA framework.

2.2 Preselection

All jets are calibrated using the corresponding routines from ATLFATB [8]. Events are selected if they contain

- at least one lepton (electron or muon) with $p_T > 20$ GeV and $|\eta| < 2.5$,
- at least six jets with $p_T > 20$ GeV and $|\eta| < 5$. At least four of these jets must be labeled as b-jets.

The p_T threshold for leptons and jets has been increased compared to the PHYSICS TDR. In addition, the jet calibration in ATLFATB has been updated since the TDR analysis, and all events are produced using CTEQ5L parton distribution functions.

2.3 Reconstruction of the final state

2.3.1 Reconstruction of $W \rightarrow \ell \nu$

To reconstruct the leptonic W decay, one needs to reconstruct the z-component of the neutrino momentum. In contrast to p_ν^x and p_ν^y , which are identified with p_{miss}^x and p_{miss}^y , one cannot directly measure p_ν^z in the detector. Instead, it can be calculated by constraining the invariant mass of the lepton-neutrino-system to the W mass. So the missing part of the neutrino momentum is obtained by solving Equation (1) for p_ν^z .

$$m_W^2 = (E_\nu + E_\ell)^2 - (p_\nu^x + p_\ell^x)^2 - (p_\nu^y + p_\ell^y)^2 - (p_\nu^z + p_\ell^z)^2. \quad (1)$$

Solving this equation results in 0, 1 or 2 solutions. Events are kept only if there exists at least 1 solution.

2.3.2 Reconstruction of $W \rightarrow jj$

To reconstruct the hadronic W decay, a list of jet-jet-pairs is formed. Only jets which are not labeled as b-jets, and which have $p_T > 20$ GeV are taken into account. In the list, only jet-jet-pairs with $m_{jj} = m_W \pm 25$ GeV are kept. For all jet-jet-pairs which fulfill these requirements, the jet four-momenta are rescaled so that m_{jj} equals m_W .

2.3.3 Reconstruction of both top decays

The two tops are reconstructed simultaneously by finding the combination of one lepton, the solution for p_ν^z , two b-jets and two non-b-jets from the list which minimizes

$$\Xi^2 = (m_{\ell\nu b} - m_t)^2 + (m_{jjb} - m_t)^2. \quad (2)$$

Events are kept if both top quark masses are inside $m_t \pm 20$ GeV.

2.3.4 Reconstruction of the Higgs decay to $b\bar{b}$

With the procedure described above, two of the b-jets are now assigned to the top decay. The remaining b-jets can then be assigned to the Higgs decay. If there are more than two b-jets left, the two with highest p_T are chosen. For these b-jets, the invariant mass m_{bb} is calculated. Events are accepted, if m_{bb} is inside $m_H^{\text{Test}} \pm 30$ GeV, where $m_H^{\text{Test}} = 120$ GeV in this study.

2.4 Results

The analysis of the $t\bar{t}H$ channel has been performed using both the FORTRAN version of the fast detector simulation and the object oriented ATHENA framework.

		FORTTRAN (%)	ATHENA (%)	TDR (%)
(1)	1 ℓ 6j(4b)	4.3	4.2	—
(2)	(single top:) > 0 sol. for p_ν^z	75.4	76.5	75.
(3)	(single top:) > 0 jj-candidates	79.2	80.2	80.
(4)	both tops reconstructed	60.1	61.2	60.
(5)	$m_{\text{j}b}$, $m_{\ell\nu b}$ inside $m_t \pm 20$ GeV	78.8	78.7	60.
(6)	m_{bb} inside $m_H \pm 30$ GeV	46.0	44.1	—
(7)	total acceptance	0.94	0.90	—

Table 2: Acceptances for the steps of the top and Higgs reconstruction in $t\bar{t}H$ events.

		FORTTRAN (%)	ATHENA (%)	TDR (%)
(1)	1 ℓ 6j(4b)	0.033	0.035	—
(2)	(single top:) > 0 sol. for p_ν^z	66.9	78.4	73.
(3)	(single top:) > 0 jj-candidates	78.1	72.1	72.
(4)	both tops reconstructed	52.0	56.4	50.
(5)	$m_{\text{j}b}$, $m_{\ell\nu b}$ inside $m_t \pm 20$ GeV	72.	73.2	60.
(6)	m_{bb} inside $m_H \pm 30$ GeV	27.	28.9	—
(7)	total acceptance	0.003	0.0042	—

Table 3: Acceptances for the steps of the top reconstruction in $t\bar{t} + X$ events.

Both have been compared in terms of acceptances for the different steps of the top reconstruction, Table 2 (signal) and Table 3 (background). To permit a comparison with the TDR report, a b-tagging parametrization with $\varepsilon_b = 0.6$, $R_c = 10$ and $R_j = 100$ was used. The ATHENA efficiencies for the background are higher than those obtained with the FORTRAN version of ATLFast, as the different multi-interaction scheme used causes a higher low P_T jet multiplicity which increases the combinatorial probability. This is compensated in the case of the signal by the cut on m_{bb} which becomes less efficient. A comparison of the efficiencies has been carried out using the same multi-interaction choice on a subsample of $t\bar{t}H$ and $t\bar{t}b\bar{b}$ (gg-fusion) events finding a good agreement.

The reconstructed masses $m_{\ell\nu b}$, $m_{\text{j}b}$ and m_{bb} are shown in Figure 3–5. Table 4 shows the mean and the variance from a Gaussian fit to the reconstructed top and Higgs mass spectra.

Table 5 gives the number of expected events for the $t\bar{t}H$ signal and $t\bar{t} + X$ background for $\mathcal{L} = 30 \text{ fb}^{-1}$. Note that the TDR numbers are for different cross sections.

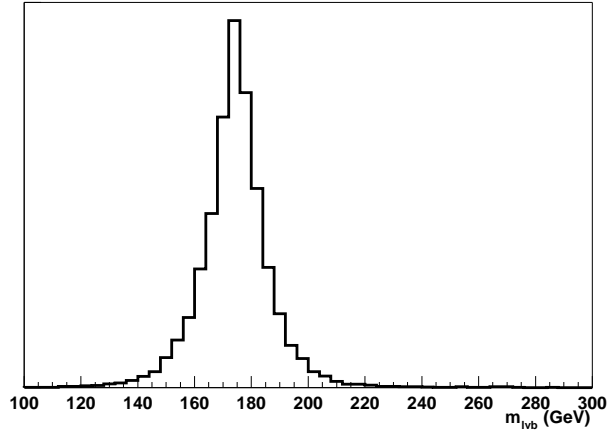


Figure 3: Reconstructed $m_{\ell\nu b}$.

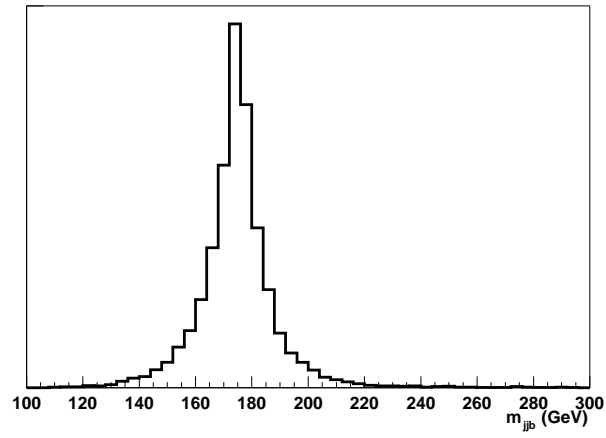


Figure 4: Reconstructed m_{jjb} .

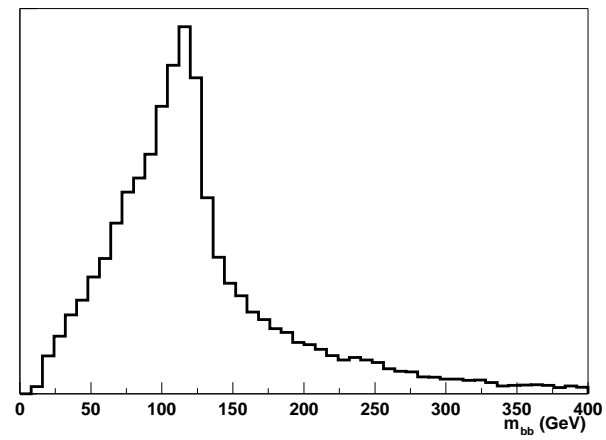


Figure 5: Reconstructed m_{bb} .

	FORTTRAN	ATHENA	TDR
$\langle m_{\ell\nu b} \rangle$ (GeV)	174	174	—
$\sigma_{m_{\ell\nu b}}$ (GeV)	8.8	8.65	8.6
$\langle m_{jjb} \rangle$ (GeV)	175	175	—
$\sigma_{m_{jjb}}$ (GeV)	7.7	6.9	9.8

Table 4: Reconstructed masses in $t\bar{t}H$ events. The numbers from the TDR are for $m_H = 100$ GeV.

	FORTTRAN	ATHENA	TDR
$t\bar{t}H$ (120)	32	32	40
$t\bar{t} + X$	144	178	120
S/\sqrt{B}	2.7	2.4	3.7

Table 5: Expected events for an integrated luminosity of 30 fb^{-1} .

3 The b-tagging performance with different detector layouts

Different b-tagging performances can be selected using the appropriate routines from ATLFASSTB. The routine ATLFBJE provides various choices for ε_b , R_c and R_j . The parameters used in many physics studies are $\varepsilon_b = 0.6$, $R_c = 10$ and $R_j = 100$. In order to study the b-tagging performance for different detector layouts, the available options of the parametrization in ATLFBJE have been extended [10]. For each detector layout, c-jet and light-jet rejections are available for $\varepsilon_b = 0.50, 0.55, 0.60, 0.65, 0.70, 0.75$ and 0.80 . Four choices for the detector layout are possible:

1. “perfect” layout (all layers, no inefficiencies beyond the ones in the pixel TDR),
2. complete layout with 2% module and 3% chip inefficiencies,
3. reduced layout (no barrel layer 1, no disk 2),
4. reduced layout with 2% module and 3% chip inefficiencies.

The parametrization is yet very preliminary, and hence not available in the official ATLFASSTB code. The inverse of the rejection as a function of the p_T is shown in Fig. 6 for the different working scenarios of the pixel detector.

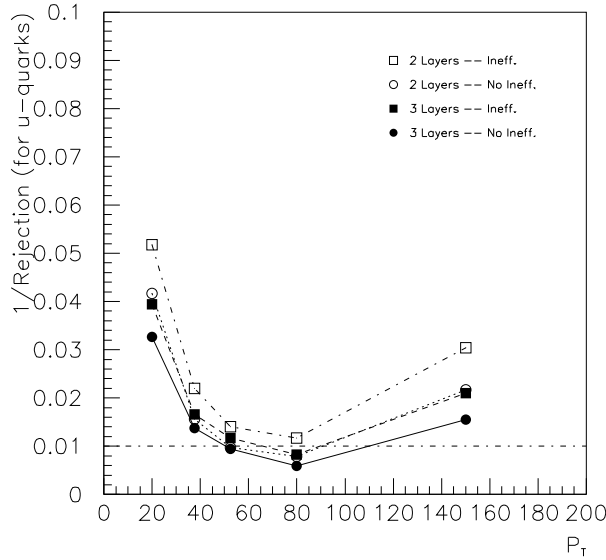


Figure 6: Inverse of the rejection as a function of the jet- p_T for $\varepsilon_b = 0.6$.

The Tables 6–8 show the number of expected events for $\mathcal{L} = 30 \text{ fb}^{-1}$ for $\varepsilon_b = 0.60$ and the different detector layouts. The number of events expected for the signal and background as a function of the layout type is sketched in

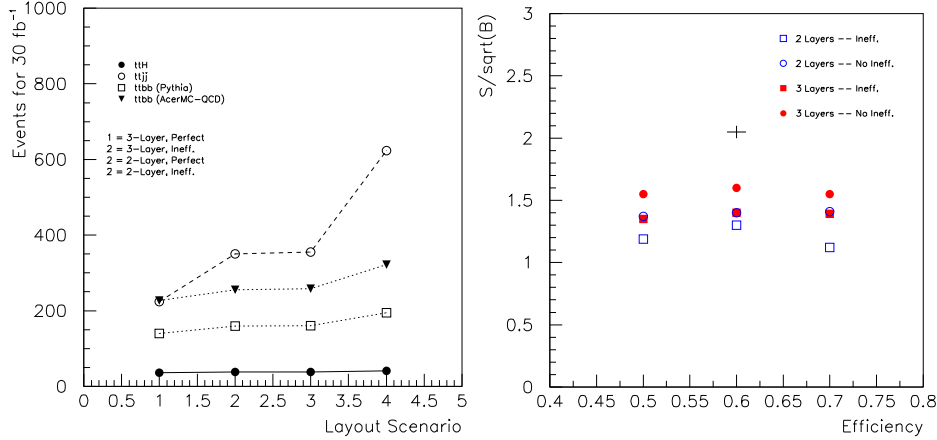


Figure 7: Left: Number of events expected in 30 fb^{-1} for the signal and the $t\bar{t}$ backgrounds, as a function of the layout considered. The PYTHIA showering approach and the ACERMC ME calculation for $t\bar{t}b\bar{b}$ events are compared. Right: The statistical significance of the signal as a function of the b-tagging efficiency for the four layout considered. The cross represents the result obtained with the TDR efficiency and rejection parametrization. The ACERMC results are used here.

Fig. 7 (left). It can be noted that the irreducible $t\bar{t}j\bar{j}$ contribution grows up faster as the layout is different from the ‘ideal’ situation. In Fig. 7 (right) the value of the significance is reported as a function of the b-tagging efficiency for the four layouts considered.

4 Conclusions

In this note the channel $t\bar{t}H$ has been re-analyzed in order to investigate the effect of a reduced layout of the pixel sub-system on the statistical significance of this channel. The reconstruction procedure of the TDR analysis was applied, and the current knowledge of the signal and background cross section was used. In addition, a new generator for the irreducible background based on matrix element calculations was integrated into the analysis.

With the same parametrization of the b-tagging performance that was used for the TDR study, we find that the statistical significance for a Higgs boson with a mass of 120 GeV is reduced from 3.6 to 2.2 assuming an integrated luminosity of 30 fb^{-1} . This change is mainly due to the smaller signal cross section and the enhanced irreducible $t\bar{t}b\bar{b}$ background predicted by the new matrix element approach.

These numbers are valid for a b-tagging efficiency of 60% and rejection factors $R_c = 10$ and $R_j = 100$ which are taken to be *p_T-independent*. Using

$\varepsilon_b = 0.5$										
FORTRAN										
1	2	3	4	5	6	7	8	9	10	11
Layout	NSET	$t\bar{t}H$	$t\bar{t}b\bar{b}$ (P)	$t\bar{t}b\bar{b}$ (A)	$t\bar{t}jj$	$t\bar{t}b\bar{b}$ (EW)	$\sum B(P)$	S/\sqrt{B}	$\sum B(A)$	S/\sqrt{B}
Complete, no ineff.	15	17.0	44.2	79.7	26.3	9.5	79.9	1.90	115.4	1.58
Complete, with ineff.	22	17.4	52.5	90.1	47.3	10.6	110.5	1.66	148.1	1.43
Reduced, no ineff.	29	17.5	51.4	89.6	48.2	10.6	110.1	1.67	148.4	1.44
Reduced, with ineff.	36	19.2	63.7	107.2	95.1	12.4	171.2	1.47	214.7	1.31

$\varepsilon_b = 0.5$										
ATHENA										
Layout	NSET	$t\bar{t}H$	$t\bar{t}b\bar{b}$ (P)	$t\bar{t}b\bar{b}$ (A)	$t\bar{t}jj$	$t\bar{t}b\bar{b}$ (EW)	$\sum B(P)$	S/\sqrt{B}	$\sum B(A)$	S/\sqrt{B}
Complete, no ineff.	15	16.2	45.	91.9	30.	10.	85.	1.76	131.9	1.41
Complete, with ineff.	22	16.9	54.	106.8	53.	12.	119.	1.55	171.8	1.29
Reduced, no ineff.	29	16.8	53.	104.6	51.	12.	116.	1.56	167.6	1.30
Reduced, with ineff.	36	18.2	66.	128.8	108	15.	189.	1.32	251.8	1.15

Table 6: Impact of the different detector layouts on the number of expected events for signal and background. The numbers have been obtained for $\varepsilon_b = 0.5$. The numbers for the QCD-process $t\bar{t}b\bar{b}$ are given in column 4 for PYTHIA, and in column 5 for ACERMC. Accordingly, the total background in column 8 is the sum of column 4, 6 and 7, and the value of column 10 is the sum of column 5, 6 and 7.

$\varepsilon_b = 0.6$										
FORTRAN										
1	2	3	4	5	6	7	8	9	10	11
Layout	NSET	$t\bar{t}H$	$t\bar{t}b\bar{b}$ (P)	$t\bar{t}b\bar{b}$ (A)	$t\bar{t}jj$	$t\bar{t}b\bar{b}$ (EW)	$\sum B(P)$	S/\sqrt{B}	$\sum B(A)$	S/\sqrt{B}
TDR parameters	5	31.8	97.0	146.6	46.9	18.2	162.0	2.50	211.7	2.19
Complete, no ineff.	17	36.4	136.8	199.3	206.5	23.5	366.9	1.90	429.4	1.76
Complete, with ineff.	24	38.3	154.9	228.3	326.1	26.5	507.5	1.70	580.9	1.59
Reduced, no ineff.	31	38.8	158.1	232.0	331.3	26.7	516.0	1.71	590.0	1.60
Reduced, with ineff.	38	41.7	191.0	273.8	589.9	31.5	812.4	1.46	895.2	1.39

$\varepsilon_b = 0.6$										
ATHENA										
Layout	NSET	$t\bar{t}H$	$t\bar{t}b\bar{b}$ (P)	$t\bar{t}b\bar{b}$ (A)	$t\bar{t}jj$	$t\bar{t}b\bar{b}$ (EW)	$\sum B(P)$	S/\sqrt{B}	$\sum B(A)$	S/\sqrt{B}
TDR parameters	5	32.0	102.	186.5	76.	22.	200.	2.26	284.5	1.90
Complete, no ineff.	17	35.2	142.	254.6	242.	29.	413.	1.73	525.6	1.54
Complete, with ineff.	24	37.3	162.	299.3	373.	33.	568.	1.57	705.3	1.40
Reduced, no ineff.	31	37.5	163.	299.4	380.	34.	577.	1.56	713.4	1.40
Reduced, with ineff.	38	41.0	205.	371.7	657.	40.	902.	1.37	1068.7	1.25

Table 7: Same as Table 6, but for $\varepsilon_b = 0.6$

$\varepsilon_b = 0.7$										
FORTRAN										
1	2	3	4	5	6	7	8	9	10	11
Layout	NSET	$t\bar{t}H$	$t\bar{t}b\bar{b}$ (P)	$t\bar{t}b\bar{b}$ (A)	$t\bar{t}jj$	$t\bar{t}b\bar{b}$ (EW)	$\sum B(P)$	S/\sqrt{B}	$\sum B(A)$	S/\sqrt{B}
Complete, no ineff.	19	71.1	354.8	459.5	1168.6	52.2	1575.6	1.79	1680.3	1.74
Complete, with ineff.	26	76.0	415.4	530.0	1829.9	59.3	2304.5	1.58	2419.2	1.54
Reduced, no ineff.	33	76.0	413.1	524.3	1779.6	58.8	2251.4	1.60	2362.7	1.56
Reduced, with ineff.	40	83.9	560.2	699.8	3619.4	75.4	4255.0	1.29	4394.5	1.27

$\varepsilon_b = 0.7$										
ATHENA										
Layout	NSET	$t\bar{t}H$	$t\bar{t}b\bar{b}$ (P)	$t\bar{t}b\bar{b}$ (A)	$t\bar{t}jj$	$t\bar{t}b\bar{b}$ (EW)	$\sum B(P)$	S/\sqrt{B}	$\sum B(A)$	S/\sqrt{B}
Complete, no ineff.	19	69.3	351.	635.0	1384.	74.	1809.	1.63	2093.0	1.51
Complete, with ineff.	26	74.9	432.	769.6	2178.	86.	2696.	1.44	3033.6	1.36
Reduced, no ineff.	33	74.8	418.	756.5	2088.	84.	2590.	1.47	2928.5	1.38
Reduced, with ineff.	40	80.9	606.	1111.7	4570.	120.	5296.	1.11	5801.7	1.06

Table 8: Same as Table 6, but for $\varepsilon_b = 0.7$

NSET	ε_b	R_c	R_j	Description
15	0.5	10.4	221.1	Complete, no ineff.
22	0.5	7.5	159.5	Complete, with ineff.
29	0.5	7.4	165.2	Reduced, no ineff.
36	0.5	5.2	110.7	Reduced, with ineff.
5	0.6	10	100	TDR
17	0.6	5.3	73.2	Complete, no ineff.
24	0.6	4.0	55.8	Complete, with ineff.
31	0.6	4.0	55.4	Reduced, no ineff.
38	0.6	2.9	40.3	Reduced, with ineff.
19	0.7	3.2	25.2	Complete, no ineff.
26	0.7	2.4	19.1	Complete, with ineff.
33	0.7	2.6	20.5	Reduced, no ineff.
40	0.7	1.4	14.3	Reduced, with ineff.
21	0.8	1.3	7.6	Complete, no ineff.
28	0.8	1.3	6.0	Complete, with ineff.
35	0.8	1.3	6.5	Reduced, no ineff.
42	0.8	1.3	5.9	Reduced, with ineff.

Table 9: Keys to the NSET values. The numbers for R_c and R_j are the nominal rejection factors, which are further multiplied by p_T -dependent scale factors.

the recent p_T -dependent b-tagging parametrization which were derived from the current layout of the ATLAS detector the significance for the same b-tagging efficiency decreases to 1.8 (1.6 when module and chip inefficiencies are taken into account). The impact of a reduced layout of the pixel subsystem has been quantified to decrease these significances by about 12%.

5 Acknowledgments

We would like to thank Jean-Baptiste de Vivie and Sasha Rozanov for providing us the b-tagging parametrization and for explaining us how to use them. We would like to thank Ian Hinchliffe for useful discussion and suggestions.

References

- [1] ATLAS detector and physics performance, Technical Design Report, CERN/LHCC/99-15.
- [2] T. Sjöstrand, L. Lönnblad, S. Mrenna, Pythia 6.2 physics and manual, hep-ph/0108264.
- [3] B. P. Kersevan, E. Richter-Was, The Monte Carlo Event Generator AcerMC 1.0 with Interfaces to PYTHIA 6.2 and HERWIG 6.3., hep-ph/0201302.
- [4] Ask Ian...
- [5] E. Richter-Was, M. Sapinski, Search for the SM and MSSM Higgs boson in the $t\bar{t}H$, $H \rightarrow b\bar{b}$ channel, ATL-PHYS-98-132.
- [6] A. Djouadi, J. Kalinowski, M. Spira, Comput. Phys. Commun. **108** (1998) 56 [hep-ph/9704448];
M. Spira, Fortschr. Phys. **46** (1998) 203.
- [7] M. Spira, the HQQ program, <http://www.desy.de/~spira/hqq/>
- [8] E. Richter-Was, D. Froidevaux, L. Poggioli, ATLFAST 2.0: A fast simulation package for ATLAS, ATL-PHYS-98-131.
- [9] W. Beenakker *et al.*, Higgs radiation off top quarks at the Tevatron and the LHC, Phys. Rev. Lett. **87** (2001) 2018058 [hep-ph/0107081];
L. Reina, S. Dawson, D. Wackeroth, Associated Higgs boson production with heavy quarks at hadron colliders: Impact of NLO results, hep-ph/0110299.
- [10] J.-B. de Vivie and A. Rozanov, private communication.